Structural and functional plasticity in the somatosensory cortex of chronic stroke patients

Judith D. Schaechter,[1,2] Christopher I. Moore,[3] Brendan D. Connell,[1,2]
Bruce R. Rosen[1,2] and Rick M. Dijkhuizen[1,2,4]

[1]MGH/MIT/HMS Athinoula A. Martinos Center for Biomedical Imaging, Charlestown, [2]Department of Radiology, Harvard Medical School, Boston, [3]Department of Brain and Cognitive Sciences and McGovern Institute for Brain Research, Massachusetts Institute of Technology, Cambridge, MA, USA and [4]Image Sciences Institute, University Medical Center Utrecht, Utrecht, The Netherlands

Correspondence to: Judith D. Schaechter, PhD, MGH/MIT/HMS Athinoula A. Martinos Center for Biomedical Imaging, 13th Street, Building 149, Room 2301, Charlestown, MA 02129, USA
E-mail: judith@nmr.mgh.harvard.edu

Animal studies have demonstrated that motor recovery after hemiparetic stroke is associated with functional and structural brain plasticity. While studies in stroke patients have revealed functional plasticity in sensorimotor cortical areas in association with motor recovery, corresponding structural plasticity has not been shown. We sought to test the hypothesis that chronic hemiparetic stroke patients exhibit structural plasticity in the same sensorimotor cortical areas that exhibit functional plasticity. Functional MRI during unilateral tactile stimulation and structural MRI was conducted in chronic stroke patients and normal subjects. Using recently developed computational methods for high-resolution analysis of MRI data, we evaluated for between-group differences in functional activation responses, and cortical thickness of areas that showed an enhanced activation response in the patients. We found a significant ($P < 0.005$) increase in the activation response in areas of the ventral postcentral gyrus (POG) in the patients relative to controls. These same ventral POG areas showed a significant ($P < 0.05$) increase in cortical thickness in the patients. Control cortical areas did not show a significant between-group difference in thickness or activation response. These results provide the first evidence of structural plasticity co-localized with areas exhibiting functional plasticity in the human brain after stroke.

Introduction

Hemiparesis is the most common acute deficit after stroke. While most patients experience partial recovery of motor function, stroke remains a leading cause of chronic disability in modern society. Motor recovery after experimental stroke in animals has been associated with reorganized neural activity (i.e. functional plasticity) in sensorimotor cortical areas (Nudo and Milliken, 1996; Dijkhuizen et al., 2001) that also exhibit morphological changes (i.e. structural plasticity) (Jones and Schallert, 1992; Stroemer et al., 1995; Li et al., 1998; Carmichael et al., 2001; Wei et al., 2001; Zhang et al., 2002). Further, co-localized functional and structural plasticity has been observed in the rat motor cortex after prolonged exercise (Swain et al., 2003) and motor learning

(Kleim et al., 2002), and in the somatosensory cortex after altered somatosensory experience (Hickmott and Steen, 2005). Collectively, these studies have led to the hypothesis that coupled functional and structural plasticity in the brain underlies post-stroke motor recovery. Studies in stroke patients have observed functional plasticity during the process of motor recovery after stroke, similar to that described in animal stroke models (Schaechter, 2004; Ward, 2005). However, to our knowledge no study has examined whether structural plasticity occurs in concert with functional plasticity in the human brain after stroke.

Recent developments in computational methods for analysing magnetic resonance images have enabled

high-resolution functional and structural analysis of the human brain. These methods permit highly accurate localization of cortical activation (Dale *et al.*, 1999; Fischl *et al.*, 1999*a*, *b*) and precise measurement of cortical thickness (Fischl and Dale, 2000; Han *et al.*, 2006). Using these computational methods following combined functional and structural MRI, we tested the hypothesis that chronic hemiparetic stroke patients exhibit structural plasticity in the same sensorimotor cortical areas that exhibit functional plasticity. Our examination of functional and structural changes in patients widens the lens towards a complete understanding of the restorative mechanisms occurring in the human brain after stroke, which will ultimately serve in the development of new post-stroke interventions that maximize motor recovery.

Material and methods
Nine patients with a chronic stroke, former in-patients of the Spaulding Rehabilitation Hospital, were enrolled (Table 1). Entry criteria included (i) an ischaemic stroke incurred ≥1 year earlier that spared the precentral gyrus (PRG) and postcentral gyrus (POG) based on MRI; (ii) stroke restricted to the left hemisphere, a criterion applied to increase patient homogeneity because brain plasticity after stroke may differ depending on hemisphere (Zemke *et al.*, 2003); (iii) acute loss of right-hand strength to ≤4 on the Medical Research Council (MRC) scale (0–5, 5 = normal) (Medical Research Council, 1976) based on physician notes entered into the medical record of the initial hospitalization within ~24 h after stroke; (iv) no prior or subsequent symptomatic stroke; (v) no impairment in detecting the tactile stimulus to be used during functional MRI—punctate contact of a 60 g Semmes–Weinstein monofilament (North Coast Medical, Inc., San Jose, CA) to the glabrous surface of the middle phalanx of right third digit (D3)—tested using an adaptive psychophysical algorithm (see below); and (vi) language and cognitive status sufficient to allow full cooperation with study procedures.

Further characterization of the enrolled patients included as follows: (i) motor (MRC scale) and somatosensory (rated as intact or impaired) status of their right upper limb acutely after stroke, based on data extracted from the initial stroke hospitalization medical records; and (ii) premorbid hand dominance using the Edinburgh Inventory laterality quotient (LQ) scale [range = −100% (strongly left-handed) to 100% (strongly right-handed)] (Oldfield, 1971), evaluated by asking the patients to recall their hand preference prior to stroke. At the time of enrolment, all patients had completed standard in-patient and out-patient post-stroke rehabilitation. In addition, three patients (#2, 5 and 7) had received supplemental out-patient therapy aimed at improving right upper limb function as participants of other research studies during the chronic stroke phase. These additional therapies were completed at least 2 months prior to participation in the current study (range 2–49 months).

Nine control subjects with no history of stroke and a normal neurological examination were also enrolled. These subjects were relatively well matched to the stroke patients with regard to age (mean = 60 years, SD = 12 years; range 36–72 years), gender (2 females, 7 males) and hand dominance (LQ mean = 81%, SD = 21%) (Oldfield, 1971).

All subjects provided written informed consent in accordance with the Human Subjects Committee of the Partners Institutional Review Board.

Sensorimotor function testing
Upper limb motor function was tested using three measures. The upper limb motor component of the Fugl-Meyer Stroke Scale (FMSS; 0–66, 66 = normal) (Fugl-Meyer *et al.*, 1975) was used to test the overall level of motor function of the right (affected side of patients) upper limb. A computerized dynamometer (Cramer *et al.*, 1997*a*) was used to determine grip strength of the right and left hand, defined as the mean peak force of 2 × 5 s trials. Grip strength of the right hand was normalized, by per cent, to that of the left hand (right force/left force × 100). The timed Jebson Hand Function Test (JHFT) was used to test function of the right and left hands; 5 of the original 7 subtests (turning cards, moving small objects, stacking checkers, moving empty can, moving full cans) were

Table 1 Patient characteristics

Patient	Age (year)	Gender	Premorbid hand dominance (LQ, %)	Time post-stroke (year)	Acute status		Lesion	
					UL (hand) MRC Score	UL somatosensation	Location	Volume (cm^3)
1	73	M	71	3.3	2–4 (0)	Intact	L pons	1.7
2	38	F	100	2.9	0–3 (0)	Intact	L posterior limb IC, medial temporal lobe	6.9
3	64	M	100	4.5	0–2 (0)	Intact	L pons	6.9
4	65	M	90	2.5	0 (0)	Intact	L pons/midbrain	9.3
5	44	M	81	1.3	0 (0)	Impaired	L inferior frontal lobe, BG, IC	64.3
6	56	M	100	2.0	0 (0)	Impaired	L inferior frontoparietal lobes, temporal lobe, BG, IC, CR	125.4
7	58	F	−4	10.2	2–3 (0)	Intact	L CR, BG, IC	5.1
8	81	M	90	1.0	0 (0)	Intact	L posterior limb IC, CR	1.1
9	59	M	82	2.0	0 (0)	Impaired	L posterior limb IC, CR	11.5
Summary	60 ± 13	2F/7M	79 ± 33	3.3 ± 2.8				

M, male; F, female; L, left; LQ, laterality quotient, a handedness measure [range = −100% (strongly left-handed) to 100% (strongly right-handed)]; UL, upper limb; IC, internal capsule; BG, basal ganglia; CR, corona radiata. UL MRC scores are strength measures (scale 0–5, 0 = no power, 5 = normal) for all muscles of the right (affected) upper limb reported in the medical record; value in parenthesis is the reported MRC score for the hand muscles; summary values are given as mean ± standard deviation.

applied, based on prior recommendations (Stern, 1992). JHFT times of the right hand were normalized, by per cent, to that of the left hand (left time/right time × 100). Patients unable to perform the JHFT subtests with the affected hand were given a score of 0%. A composite motor function score for each patient was determined by entering all patients' motor function data into a principal component analysis using MATLAB (The Mathworks, v6.5.1). The first principal component, which accounts for the greatest percentage of the variability within the data, was taken as the score representing motor outcome for each patient. We examined relationships between the motor outcome scores and the MRI-based measures of functional and structural plasticity across the patients.

Tactile sensitivity was tested at the glabrous surface of the middle phalanx of the right and left D3 using Semmes–Weinstein monofilaments. Testing was conducted using an adaptive psychophysical algorithm (Simpson, 1989) for 40 trials per digit, with the tactile detection threshold determined as the force perceived with 80% accuracy.

MRI

MRIs were acquired using a 3T Siemens Allegra magnetic resonance scanner and a quadrature head coil. With the subject supine, cushions were packed around the head to limit its motion, and splints were used to immobilize the forearms (in pronation) and hands (digits in extension) off the abdominal area. The splints were fabricated with an opening to permit access to the glabrous surface of the middle phalanx of D3. Two structural volumes were collected using a T1-weighted MPRAGE sequence [repetition time (TR) = 7 ms; echo time (TE) = 3 ms; flip angle (α) = 7°; field-of-view (FOV) = 256 × 256 mm; matrix size = 192 × 256; effective slice thickness = 1.33 mm]. In stroke patients, T2-weighted turbo spin-echo images (TR = 10 s; TE = 65 ms; α = 120°; FOV = 210 × 210 mm; matrix size = 256 × 256; slice thickness = 5 mm; interslice gap = 1 mm; number of slices = 20) were collected. Blood oxygenation level-dependent (BOLD) functional images were collected using a T2*-weighted gradient-echo, echo planar imaging sequence (TR = 2 s; TE = 30 ms; α = 90°; FOV = 200 × 200 mm; matrix size = 64 × 64) with slices (thickness = 5 mm; interslice gap = 1 mm; number = 20; number of acquisitions/slice = 130) parallel to the anterior commissure–posterior commissure line. Functional images were collected during periods of passive tactile stimulation (6 × 20 s) alternating with periods of no stimulation (7 × 20 s). We opted to employ passive tactile stimulation, rather than an active motor task, because the former allowed us to probe sensorimotor functional representations (Moore *et al.*, 2000) of the affected hand in patients who represent a wide range of residual motor impairment. Punctate tactile stimulation was delivered manually by an investigator over the glabrous surface of the middle phalanx of D3 by means of a Semmes–Weinstein monofilament (60 g), paced at 3 Hz by a computer-generated (MacStim, version 2.6) metronome presented to the investigator only. Four functional runs were collected during unilateral D3 stimulation (two right D3, two left D3) to each subject. The side of stimulation during collection of the first functional run was randomized across subjects, and the side of stimulation during subsequent functional runs in each subject alternated between sides. Subjects were instructed to keep their eyes closed, their entire body relaxed and to pay close attention to the tactile sensation at their digit.

Image analysis

FreeSurfer software (http://surfer.nmr.mgh.harvard.edu) was used for all functional and structural image analysis, with the exception of Alice software (Hayden Image Processing Solutions, Denver, CO, USA) that was used to determine the location and volume of the lesion based on the T2-weighted images acquired from the patients. Lesion volume was determined by an experienced neuroradiologist who manually outlined the T2 abnormality slice by slice.

Visual inspection of the two sets of T1-weighted MPRAGE structural images from each subject revealed no motion artefacts. The two structural volumes from each subject were motion-corrected using a 6-parameter (3 translations, 3 rotations) rigid-body transformation, intensity-normalized, then averaged to create a single structural volume with high contrast-to-noise. Cortical surfaces from each subject were reconstructed using an automated procedure that involved white matter segmentation, then tessellation of the identified grey/white matter boundary and pial surfaces, as described in detail previously (Dale *et al.*, 1999). Visual inspection of the reconstructed surfaces in the central sulcus region (within our primary region-of-interest) on each subject's structural volume revealed no abnormalities (data not shown).

The cortical surface model from each subject was spatially normalized to a spherical surface template using a procedure that optimally aligns major cortical sulci and gyri (Fischl *et al.*, 1999*a*). Cortical surface models from all study subjects were averaged to provide a group-average cortical surface model that best accounts for the topological variability of the subjects in this study (Fischl *et al.*, 1999*b*).

We tested whether the spatial alignment of each subject's cortical surface model to the spherical surface template was accurate even in brains spatially distorted by a stroke. Visual inspection revealed accurate mapping of the template's central sulcus region to each subject's cortical surface model, including surface models from patients with a large stroke (data not shown). Further, there were no significant ($P > 0.05$, two-tailed, unpaired Student's *t*-test) between-group differences in the per cent overlap of the template's central sulcus region to the central sulcus on the left (lesioned hemisphere of patients) or right cortical surface models (left—patients: 63 ± 2%, controls: 65 ± 2%; right—patients: 74 ± 2%, controls: 75 ± 2%). These findings exclude misalignment of the cortical surface models across subjects as responsible for the between-group differences in the BOLD activation response and cortical thickness found in this study (Results section).

Thickness across the cortical mantle was computed in the structural volume for each subject using an automated procedure that measures the shortest distance between vertices of the grey/white matter boundary and pial surfaces, as described previously (Fischl and Dale, 2000). As this method uses signal intensity and continuity information, the thickness measurements can achieve an accuracy of at least an order of magnitude greater than the voxel dimensions of the raw MRI data used to generate the cortical surface reconstructions. This automated method has been shown to be highly reliable (Han *et al.*, 2006), and has been validated histologically and manually in pathological and aged human brains (Rosas *et al.*, 2002; Kuperberg *et al.*, 2003; Salat *et al.*, 2004). The thickness measurements from each subject were spatially normalized into the spherical surface-based coordinate system (Fischl *et al.*, 1999*a*).

Functional images from each subject were co-registered with their structural volume using a rigid-body transformation. The functional data were motion-corrected using a 6-parameter (3 translations, 3 rotations) rigid-body transformation, intensity-normalized and spatially smoothed using a 3D Gaussian kernel [full-width at half maximum (FWHM) = 3 mm]. Each subject's functional data from replicate runs collected during unilateral D3 tactile stimulation were

concatenated, and the average signal intensity and standard deviation of the residual error were estimated at each voxel for each condition. These voxel-based signal intensity maps were spatially normalized into the spherical surface-based coordinate system (Fischl *et al.*, 1999*a*).

In order to test the hypothesis that structural plasticity co-localizes with functional plasticity in sensorimotor cortical areas in stroke patients, we empirically identified regions-of-interest exhibiting functional plasticity in the patients. Functionally defined regions-of-interest were determined as follows. A general linear model was fitted at each vertex across the cortical surface. The general linear model included a low-frequency drift term, as well as motion-correction parameters as nuisance regressors. The haemodynamic response to unilateral D3 stimulation was modelled as a gamma function (delta = 2.25 s, tau = 1.25 s) (Dale and Buckner, 1999) convolved with a boxcar function. The difference in the BOLD activation response between the patient and control groups was estimated at each vertex, with subject regarded as a fixed effect. A fixed-effects model was used at this stage of the analysis because the vertex-to-vertex correspondence in the D3 functional fields might be relatively low due to differences in sensorimotor experience and/or stroke across the subjects. The between-group difference maps were corrected for multiple comparisons by controlling the false discovery rate (Genovese *et al.*, 2002) to 1%, and the minimum cluster surface area to 50 mm^2. Surviving clusters of the difference maps became candidate regions-of-interest. In order to guard against our functionally defined regions-of-interest being driven by outliers, we then tested more stringently for between-group differences in the BOLD activation response in the candidate regions-of-interest using a random-effects model. The raw time-course of the BOLD activation response (in per cent signal change from baseline) was averaged across all vertices of each region-of-interest for each subject. The average time-course was used to compute the mean BOLD activation response occurring from the completion of the rising phase (6 s after stimulation onset) to the end of the stimulation (20 s after stimulation onset). For each candidate region-of-interest, the mean BOLD activation response from all subjects was entered into a two-tailed, unpaired Student's *t*-test to test for between-group differences in functional activation. Finally, regions-of-interest that exhibited a between-group difference in the mean BOLD activation response at an alpha level of 0.05 became the functionally defined regions-of-interest used in further analyses.

We observed that the functionally defined regions-of-interest traversed distinct somatosensory cortical areas (Results section) based on prior anatomical and physiological studies in monkeys and humans (Kaas, 1983; Jones, 1986; Brodmann, 1994; Geyer *et al.*, 1999; Grefkes *et al.*, 2001). Accordingly, our primary regions-of-interest were subdivided into areas corresponding to putative area 3b (residing in the posterior wall of the central sulcus), putative area 1 (residing in the crown of the POG) and putative area 2 (residing in the anterior wall of the postcentral sulcus). Neurons of area 3b, considered the primary somatosensory cortex based on anatomical and physiological criteria, have been shown to possess discrete tactile receptive fields. Area 1 neurons have been shown to possess tactile receptive fields that are more complex than those in area 3b. Area 2 neurons have been shown to be responsive to tactile and proprioceptive stimulation and have complex receptive field properties. These secondary regions-of-interest were delineated on the group-average cortical surface model to best account for topographical variability across the subjects. We tested our hypothesis that

structural plasticity co-localizes with areas of functional plasticity in chronic stroke patients by evaluating the mean BOLD activation response (6–20 s post-stimulation onset) and mean cortical thickness in these secondary regions-of-interest.

Between-group differences in cortical thickness in our functionally defined regions-of-interest could potentially result from differences in the gradient of T1 signal intensity in tissue bordering the cortex, which could cause the surface reconstruction algorithm to incorrectly localize the grey/white matter boundary and pial surfaces. To address this possibility, we tested for between-group differences in change in mean T1 signal intensity of tissue 10% above and below the normalized distance between the two reconstructed surfaces of our functionally defined regions-of-interest using two-tailed, unpaired Student's *t*-tests. We found no significant ($P > 0.05$) differences in signal intensity change across the grey/white matter boundary or pial surfaces for our functionally defined regions-of-interest in the patients relative to controls (data not shown). This finding excludes differential localization of the grey/white matter boundary and pial surfaces in the structural volume as responsible for the between-group differences in cortical thickness we observed in our functionally defined regions-of-interest (Results section).

To test the selectivity of structural changes co-localized with areas of functional plasticity, we also evaluated mean cortical thickness (and mean BOLD activation response to contralateral D3 tactile stimulation) in two sets of control cortical areas. The first set of control cortical areas was selected as being topographically related to our functionally defined regions-of-interest, while respecting known anatomical and physiological distinctions. Each topographically defined control region-of-interest was a circle with a surface area that approximated the mean surface area of our functionally defined regions-of-interest. The second set of control cortical areas was commonly activated in the patients and controls in response to tactile stimulation to the right (affected side of patients) D3. The functionally defined control regions-of-interest were determined by estimating the average BOLD activation response across all the subjects at each vertex, with subject regarded as a random effect. The average activation map was thresholded by imposing a probability level of 0.001 at each vertex and a minimum cluster surface area of 50 mm^2. We excluded from the thresholded, average activation map the functionally defined regions-of-interest that exhibited a between-group difference in the BOLD activation response. The resultant activation map was subdivided based on known anatomical and physiological distinctions to achieve functionally defined control regions-of-interest.

Statistical analysis

StatView (version 4.5) was used for statistical procedures. Between-group differences in sensorimotor function were analysed using the two-tailed, unpaired Student's *t*-test, with the exception of one motor function measure for which the Mann–Whitney *U*-test was applied because the scores from the controls were not normally distributed. Separate two-way, mixed-model analysis of variance (ANOVA), with group (patients, controls) as the between-subjects factor and cortical area as the within-subjects factor, was used to test for main and interaction effects of the factors on activation response and cortical thickness. We point out that the level of significance of a main effect of group on activation response in the cortical areas is inflated because the functionally defined regions-of-interest were explicitly selected because they exhibited significant between-group differences in activation response. On the other

hand, the level of significance of a main effect of group on cortical thickness is valid because the cortical areas were selected independent of the thickness measurements. Relationships between activation response and cortical thickness in functionally defined and control regions-of-interest in the patients and controls were evaluated using the Pearson correlation coefficient, uncorrected for multiple comparisons. In patients, additional relationships between motor outcome, using the first principal component of the motor function scores, versus thickness and versus activation were evaluated using the Pearson correlation coefficient (uncorrected). A difference in activation response between patients with good versus poor motor outcome (dichotomized based on the first principal component of the motor function scores) was tested using the Mann–Whitney U-test. Alpha was set to 0.05 for all statistical tests. Results are expressed as the mean ± SEM.

Results
Sensorimotor function
Review of patient medical records revealed that acutely after stroke the right (affected) hand had no muscle power in all nine enrolled patients, and had impaired somatosensation in three of the nine patients (Table 1).

At the time of study enrolment, formal testing revealed that the chronic stroke patients exhibited a range of upper limb motor function (Table 2). All but one patient (#8) could grip with the right (affected) hand, indicating that eight of the nine patients had made recovery of motor function of the right hand since the acute stroke. On a group basis, however, the patients had residual motor impairments of the right upper limb. Normalized grip strength was significantly reduced in the patients (patients: 50 ± 11%; controls: 113 ± 5%; $P < 0.0001$, Student's t-test). Scores on the FMSS were significantly lower in the patients (patients: 42 ± 7; controls: 66 ± 0; $P < 0.01$, Mann–Whitney U-test). The normalized time to perform functional tasks of the JHFT was significantly longer in the patients (patients: 49 ± 14%; controls: 108 ± 3%; $P = 0.001$, Student's t-test). The first principal component of the motor function measures from all of the patients accounted for 95.4% of the variability, and was taken to reflect motor outcome of each patient.

Table 2 Sensorimotor function of the right (affected) upper limb in the chronic stroke patients

Patient	Grip strength (% L)	FMSS score	JHFT (% L)	Motor outcome (1st PC)	Tactile detection threshold (g)
1	89	66	122	85	0.160
2	91	66	89	62	0.008
3	53	48	62	14	0.160
4	75	60	86	48	0.160
5	60	53	31	3	0.160
6	8	11	0	−72	2.000
7	28	33	30	−30	0.040
8	0	6	0	−78	0.160
9	43	36	21	−26	0.400

An entry of 0 indicates that the patient was unable to perform the test with the affected hand. L, left hand; PC, principal component.

The patients also exhibited a range of tactile sensitivity at the time of study enrolment (Table 2). The tactile detection threshold of the right D3 of two patients (#6 and 9) was outside the tactile detection threshold range of the right D3 of the control subjects (0.008–0.160 g). However, even with consideration given to these two patients, tactile detection thresholds were not significantly different between groups for either the right D3 (patients: 0.36 ± 0.21 g, controls: 0.09 ± 0.02; $P = 0.22$, Student's t-test) or left D3 (patients: 0.10 ± 0.02 g, controls: 0.08 ± 0.02; $P = 0.51$, Student's t-test). Further, tactile sensitivity of the right D3 of all patients was an order of magnitude greater than the strength of the tactile stimulation delivered during functional MRI (60 g), reflecting our enrolment criterion that this stimulus be detectable. This result rules out the possibility that the observed between-group differences in the BOLD activation response to the tactile stimulation (see below) were due to lack of stimulus detection in the patient group.

Functional MRI
Figure 1 shows a typical BOLD activation response pattern to unilateral tactile stimulation to D3 in a control subject. The tactile stimulation produced marked activation responses in the cortex contralateral to the stimulated hand, including the hand region of the PRG and POG, as well as ventral POG, secondary somatosensory cortex and supplementary motor area. Activation responses in the ipsilateral cortex were confined largely to the ventral POG and secondary somatosensory cortex.

Between-group difference analysis revealed that the patients exhibited a significant increase in the BOLD activation response, as compared with controls, to stimulation of the right (affected side of patients) D3 in a region of the left (ipsilesional in patients) ventral POG (304 mm^2; patients: 0.68 ± 0.12%; controls: 0.32 ± 0.07%; $P < 0.025$, Student's t-test; Fig. 2A and B). This ventral POG region did not intersect the stroke cavity in any patient. Patients also exhibited a significant increase in the activation response, as compared with controls, to stimulation of the left (unaffected side of patients) D3 in a region of the right (contralesional in patients) ventral POG (94 mm^2; patients: 0.69 ± 0.13%; controls: 0.15 ± 0.13%; $P < 0.01$, Student's t-test; Fig. 2C and D). There was no cortical region in which right or left D3 stimulation elicited a significantly stronger activation response in the controls as compared with the patients.

The ventral POG regions that exhibited a between-group difference in the BOLD activation response were further subdivided into areas corresponding to 3b (primary somatosensory cortex) and 1 and 2 (secondary somatosensory cortices), based on recognized anatomical and physiological distinctions (Kaas, 1983; Jones, 1986; Brodmann, 1994; Geyer et al., 1999; Grefkes et al., 2001). Accordingly, the left ventral POG region was divided into putative areas 3b, 1 and 2, whereas the right ventral POG region was identified
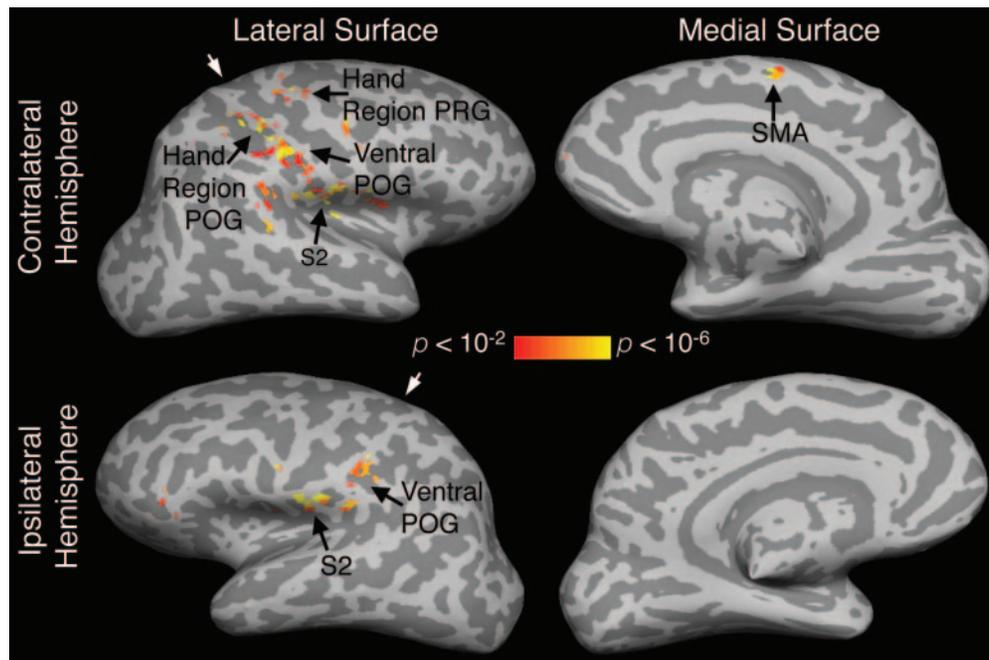
Fig. 1 Statistical activation maps obtained from functional MRI during tactile stimulation to the left D3 of a normal subject. The BOLD activation response pattern is typical for that observed in controls. The activation maps ($P < 0.01$, corrected) are displayed on the model of the subject's inflated cortical surfaces. Light grey areas of a cortical surface indicate gyri; dark grey areas indicate sulci. White arrowheads point to the central sulcus. S2, secondary somatosensory cortex; SMA, supplementary motor area.

as putative area 1 (Fig. 3A). The mean BOLD activation response in putative areas 3b, 1 and 2 was estimated in the patients and controls (Fig. 3B). An ANOVA used to test effects on the activation responses in the ventral POG areas detected a significant main effect of group [$F(1,64) = 13.03$, $P < 0.005$]; we note that this significance level is inflated because the ventral POG areas were sub-components of functionally defined regions-of-interest that were explicitly selected because they exhibited significant between-group differences in activation. This ANOVA also detected a significant main effect of cortical area [$F(3,64) = 8.12$, $P < 0.0005$], but no significant interaction between the two factors. These results indicate that the chronic stroke patients exhibited an enhanced activation response in the identified ventral POG areas. The data further show that while the magnitude of the activation response differed across the cortical areas, this was not affected by subject group.

Structural MRI

We next examined whether the chronic stroke patients exhibited structural changes in the ventral POG areas that exhibited an enhanced BOLD activation response. Figure 3C shows the mean cortical thickness of the ventral POG areas. An ANOVA conducted to test whether cortical thickness of the ventral POG areas differed between groups and across areas detected significant main effects of group [$F(1,64) = 4.69$, $P < 0.05$] and area [$F(3,64) = 28.39$, $P < 0.0001$], with no significant interaction effect. This result indicates that there

were regional differences in cortical thickness across the ventral POG areas. More importantly, they indicate that cortical thickness of the ventral POG areas was greater in the patients as compared with controls.

In order to examine whether the significant between-group difference in thickness observed in the ventral POG areas was restricted to cortical areas that also exhibited an enhanced BOLD activation response, we performed analyses on two sets of four control cortical areas—topographically defined and functionally defined. The topographically defined control cortical areas were located in the (i) anterior wall of the central sulcus (putative area 4) (Rademacher *et al.*, 2001) in the ventral PRG of the left (ipsilesional in patients) hemisphere; (ii) crown of the hand region POG (putative area 1) of the left hemisphere; (iii) left calcarine sulcus (putative area 17); and (iv) anterior wall of the central sulcus (putative area 4) in the ventral PRG of the right (contralesional in patients) hemisphere. The functionally defined control cortical areas were located in the hand region of the left POG in the (i) fundus of the central sulcus (putative area 3a) (Geyer *et al.*, 1999); (ii) posterior wall of the central sulcus (putative area 3b); (iii) crown of the POG (putative area 1); and (iv) anterior wall of the postcentral sulcus (putative area 2).

Figure 4A shows the mean cortical thickness in the two sets of control cortical areas. An ANOVA conducted to test for effects on thickness across the topographically defined control cortical areas did not detect a significant main effect of group [$F(1,64) = 0.11$, $P = 0.75$], nor a significant inter-action effect, but did detect a significant main effect of area [$F(3,64) = 101.56$, $P < 0.0001$]. A separate ANOVA conducted
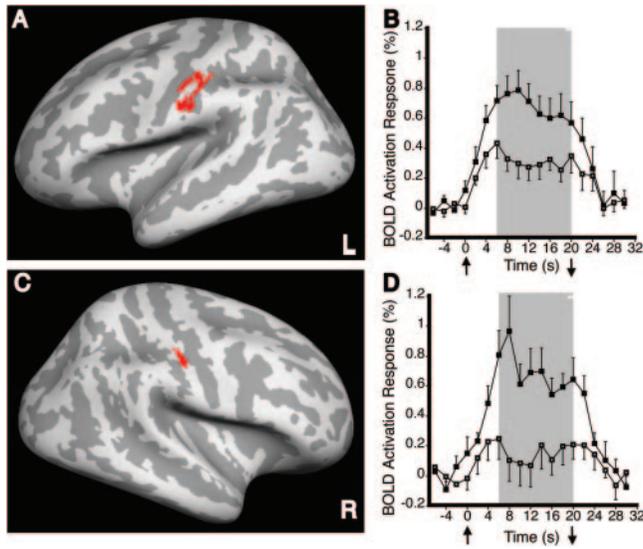
Fig. 2 Between-group differences in BOLD activation response to unilateral tactile stimulation to D3. Difference maps are displayed on the group-average, inflated cortical surface model. (**A**) Area in the left (ipsilesional in patients) ventral POG with a greater activation response in patients as compared with controls during right (affected side of patients) D3 stimulation. (**B**) Time-course of the BOLD activation response across the left, ventral POG area (red in **A**). The mean activation response was significantly ($P < 0.025$, Student's t-test) greater in patients relative to controls during the 6–20 s stimulation interval (grey bar). (**C**) Area in the right (contralesional in patients) ventral POG with a greater activation response in patients as compared with controls during left (unaffected side of patients) D3 stimulation. (**D**) Time-course of the BOLD activation response in the right, ventral POG area (red in **C**). The mean activation response was significantly ($P < 0.01$, Student's t-test) greater in patients relative to controls during the 6–20 s stimulation interval. Filled squares, patients; open squares, controls; upward arrow, stimulation onset; downward arrow, stimulation end.

to test for effects on thickness across the functionally defined control cortical areas also did not detect a significant main effect of group [$F(1,64) = 0.348$, $P = 0.56$], nor a significant interaction effect, but detected a significant main effect of area [$F(3,64) = 24.495$, $P < 0.0001$].

Figure 4B shows the mean BOLD activation response in the two sets of control cortical areas. An ANOVA conducted to test for effects on activation across the topographically defined control cortical areas did not detect a significant main effect of group [$F(1,64) = 0.09$, $P = 0.77$], nor a significant interaction effect, but did detect a significant main effect of area [$F(3,64) = 9.65$, $P < 0.0001$]. Similarly, an ANOVA conducted to test for effects across the functionally defined control cortical areas did not detect a significant main effect of group [$F(1,64) = 0.09$, $P = 0.76$], nor a significant interaction effect, but did detect a significant main effect of area [$F(3,64) = 11.77$, $P < 0.0001$].

These analyses revealed no significant between-group difference in thickness in control cortical areas that also showed no significant between-group difference in the BOLD activation response. These findings indicate that the increase
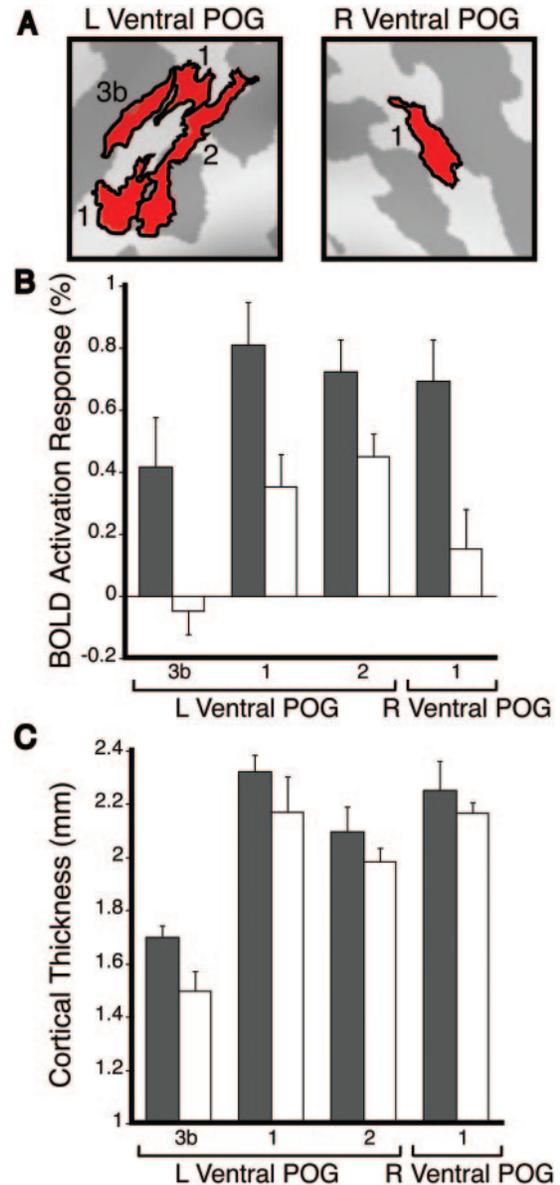
Fig. 3 Cortical thickness and BOLD activation response in putative areas of the ventral POG. (**A**) Delineation of putative areas 3b, 1 and 2 of the left (L) and right (R) ventral POG area. (**B**) Magnitude of the activation response in putative areas of the L ventral POG during right (affected side of patients) D3 stimulation, and of the R ventral POG during left D3 stimulation, in the patients and controls. A two-way, mixed-model ANOVA detected significant main effects of group [$F(1,64) = 13.03$, $P < 0.005$] and cortical area [$F(3,64) = 8.12$, $P < 0.0005$], with no significant interaction between these two factors. (**C**) Thickness of the putative ventral POG areas in the patients and controls. A two-way, mixed-model ANOVA testing effects across the ventral POG areas detected significant main effects of group [$F(1,64) = 4.69$, $P < 0.05$] and area [$F(3,64) = 28.39$, $P < 0.0001$], with no significant interaction. Grey bars, patients; white bars, controls.

in cortical thickness observed in the ventral POG areas of the patients relative to the control subjects was not generalized across the cortex, but was restricted to areas also exhibiting increases in the activation response.
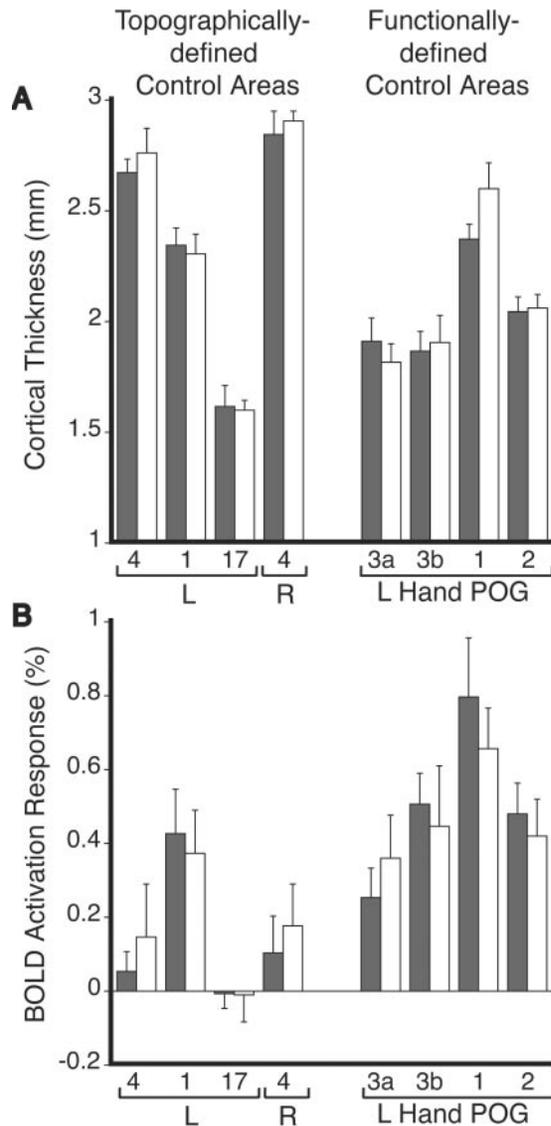
Fig. 4 Thickness and BOLD activation response in topographically defined and functionally defined control cortical areas. Topographically defined control areas were located in putative area 4 of the left (L) and right (R) ventral PRG, putative area 1 in the hand region of the L POG, and putative area 17 of the L calcarine sulcus. Functionally defined control areas were located in the hand region of the L POG. (**A**) Thickness in the two sets of control cortical areas. Separate two-way, mixed-model ANOVAs did not detect significant main effects of group, nor interaction effects, but did detect significant main effects of area [topographically defined: $F_{(3,64)} = 101.56$, $P < 0.0001$; functionally defined: $F_{(3,64)} = 24.495$, $P < 0.0001$]. (**B**) Magnitude of the activation response in the two sets of control cortical areas during tactile stimulation to the contralateral D3. Separate two-way, mixed-model ANOVAs did not detect significant main effects of group, nor interaction effects, but did detect significant main effects of area [topographically defined: $F_{(3,64)} = 9.65$, $P < 0.0001$; functionally defined: $F_{(3,64)} = 11.77$, $P < 0.0001$]. Grey bars, patients; white bars, controls.

Correlation analyses

In the patients and controls, we examined the correlation between cortical thickness and the BOLD activation response in each ventral POG area, and each control cortical area.
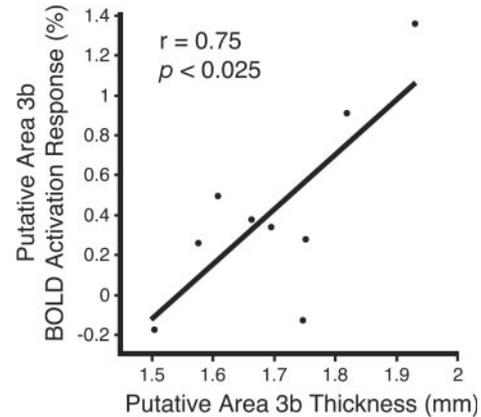
Fig. 5 Plot of relationship between cortical thickness and activation response in putative area 3b of the left (ipsilesional) ventral POG in the stroke patients.

In patients, putative area 3b of the left (ipsilesional) ventral POG exhibited a significant positive correlation between thickness and activation ($r = 0.75$, $P < 0.025$, uncorrected, Pearson correlation; Fig. 5). No other ventral POG area or control cortical area exhibited a significant correlation between thickness and activation in the patients or controls.

We also tested in the patients for relationships between motor outcome (first principal component of the motor function scores) and plasticity (activation response, cortical thickness). No significant correlation between these measures was detected. However, there was a non-significant trend toward an increase in the activation response in the left (ipsilesional) ventral POG during right (affected) D3 stimulation in patients with good motor outcome as compared with those with poor motor outcome (good: $0.81 \pm 0.18\%$, $n = 5$; poor: $0.50 \pm 0.12\%$, $n = 4$; $P = 0.086$, Mann–Whitney U-test).

Discussion

The adult human brain responds adaptively to experience and injury (Buonomano and Merzenich, 1998). Several studies have shown that recovery of motor function in patients after stroke is associated with functional reorganization in the brain (Schaechter, 2004; Ward, 2005). The present study provides the first demonstration of structural plasticity co-localized with functional plasticity in the human brain after stroke.

Structural plasticity

We found that thickness of the cortical mantle of ventral POG areas, corresponding to areas 3b, 1 and 2, was significantly greater in the chronic stroke patients relative to the control subjects. Two related results strengthen this finding. Firstly, we did not find a significant increase in thickness in control cortical areas defined either topographically or functionally, suggesting that an increase in thickness was not a generalized finding across the cortical mantle of chronic stroke patients.

Secondly, we detected significant thickness differences across distinct ventral POG and control cortical areas delineated based on known anatomical and functional criteria, which is consistent with previous reports of gyral regions of neocortex being thicker than sulcal regions (Fischl and Dale, 2000), and the anterior wall of the central sulcus being thicker than the posterior wall (Meyer *et al.*, 1996). The magnitude of the cortical thickness increase we observed in the ventral POG areas was relatively small, ranging from ∼4 to 13%, yet is comparable with the increases in cortical thickness others have found in rat motor cortex after motor skill learning (Anderson *et al.*, 2002; Kleim *et al.*, 2002), in rat visual cortex after rearing in an enriched environment (Diamond *et al.*, 1966) and in cortices of humans with specific mental disorders (Rauch *et al.*, 2004; Thompson *et al.*, 2005). Our finding is also consistent with the increased grey matter volume found in the sensorimotor cortices of professional musicians with extensive motor training relative to amateur musicians and non-musicians (Gaser and Schlaug, 2003). These previous findings, in conjunction with our result, suggest that the human sensorimotor cortex can undergo structural changes in response to sensorimotor experience and brain injury.

Given the spatial resolution and signal-to-noise of the current structural MRI data collected using a 3 T MRI scanner, the microscopic substrate of the increase in cortical thickness in the ventral POG areas was not discernible. However, previous studies suggest that neural and non-neural elements may have contributed to the cortical thickness increase we observed. In rats, an increase in cortical thickness has been shown to co-localize with an increase in the number of synapses per neuron in the motor cortex after motor training (Kleim *et al.*, 2002), and with an increase in glial number in the visual cortex after environmental enrichment (Diamond *et al.*, 1966). Experimental stroke in rats has been shown to induce synaptogenesis (Stroemer *et al.*, 1995), angiogenesis (Wei *et al.*, 2001; Zhang *et al.*, 2002), as well as increased neuronal sprouting (Li *et al.*, 1998; Carmichael *et al.*, 2001) and dendritic arborization (Jones and Schallert, 1992). Further, it has been recently shown that experimental stroke induces sequential waves of neuronal growth-promoting genes (Carmichael *et al.*, 2005). Collectively, these findings lead us to speculate that the cortical thickness increase we observed in the chronic stroke patients was associated with growth of neural elements as well as several non-neural elements that provide metabolic and structural support to the new neural elements.

Functional plasticity

Activation was increased in the ipsilesional POG ventral to the hand region in response to tactile stimulation to the affected D3 of the stroke patients as compared with controls. The location of this functional change was found in patients whose stroke location, while left-sided and sparing the PRG and POG in all cases, was otherwise fairly heterogeneous. The

reason why patients with varied lesion sites should exhibit functional plasticity in the ventral POG is unclear. However, it is notable that the ventral POG was activated in our control subjects, consistent with previous neuroimaging studies (Burton *et al.*, 1997; Burton *et al.*, 1999). This finding suggests that the ventral POG might normally play a role in higher-order processing of somatosensory information. After hemiparetic stroke, it is possible that activity in the ventral POG increases to support sensorimotor function. Ventral areas of the ipsilesional sensorimotor cortex have previously been reported to undergo functional reorganization in patients with subcortical or cortical stroke (Weiller *et al.*, 1993; Zemke *et al.*, 2003; Cramer and Crafton, 2006). Further, functional reorganization involving the ipsilesional POG associated with the stroke-affected hand has been evidenced previously as a partial (Pineiro *et al.*, 2001; Calautti *et al.*, 2003) or complete (Cramer *et al.*, 2000; Jang *et al.*, 2005) shift in the sensorimotor cortex activation toward the POG.

The functional change we observed in the ipsilesional ventral POG in the patients was associated with motor recovery of the affected hand from the time of the acute stroke to study enrolment in eight of the nine patients. However, we found only a non-significant trend toward an increased BOLD activation response in the ipsilesional ventral POG in patients with good as compared with poor motor outcome of the affected upper limb. Therefore, the enhanced activation response we observed in the ipsilesional POG was associated, but not directly correlated, with motor recovery in our patients. This result is similar to the lack of correlation between the extent of posterior shift in activation toward the POG and the level of motor recovery reported in earlier studies (Pineiro *et al.*, 2001; Calautti *et al.*, 2003). While there is growing evidence that motor recovery after stroke is related to functional reorganization of the brain (Ward, 2005), our ability to detect a significant relationship between our indices of functional plasticity and motor outcome may have been limited by several factors, such as differences among the patients in lesion site and post-stroke rehabilitation. Further, the cross-sectional design of our study limited our correlation analyses to motor function measures acquired at a single session late after stroke, rather than multiple measures acquired over time during the recovery process. Consequently, our study was well designed to detect persistent functional changes common to stroke patients, but less well designed to identify functional plasticity mechanisms tightly linked to the process of motor recovery after stroke. The observed lack of a significant relationship between motor outcome and functional activation might also reflect our use of passive tactile stimulation, rather than an active motor task, during functional MRI. Use of the passive task permitted us to enrol patients who represent a broad range of residual motor deficit. However, functional plasticity related to tactile stimulation in patients may relate only indirectly to motor outcome late after stroke. Further research is required to elucidate the precise relationship between functional plasticity in sensorimotor cortices, operating in conjunction with

structural plasticity, and the complex dynamics of reacquisition of motor function after stroke.

We also observed enhanced activation in the contralesional ventral POG associated with the unaffected hand of patients. Though less commonly studied than functional plasticity associated with the stroke-affected limb, evidence of reorganization associated with the unaffected upper limb has been observed previously in patients after unilateral stroke (Cramer *et al.*, 1997*b*; Luft *et al.*, 2004). Among the possible mechanisms to account for reorganization of the unaffected hand representation in the contralesional somatosensory cortex is a use-dependent change (Elbert and Rockstroh, 2004) resulting from increased compensatory use of the unaffected upper limb. This interpretation is supported by studies in rats that showed increased use of the non-impaired limb after a unilateral sensorimotor cortex lesion that was associated with structural changes in the contralesional sensorimotor cortex (Jones and Schallert, 1994). Another explanation is a transcallosal impact of reorganization within the ipsilesional somatosensory cortex. Direct and indirect callosal connections between hand representations within sensorimotor cortices of the two hemispheres have been demonstrated in animals (Killackey *et al.*, 1983; Krubitzer *et al.*, 1998).

Co-localized structural and functional plasticity

Ventral POG areas of the chronic stroke patients exhibited evidence of structural and functional plasticity. An increase in synaptic and capillary density may have contributed to the parallel increase in cortical thickness and BOLD activation response in these areas. Co-localized structural and functional plasticity has been observed previously in sensorimotor cortical areas of animals in response to manipulations of sensorimotor experience (Kleim *et al.*, 2002; Swain *et al.*, 2003; Hickmott and Steen, 2005), and has been implicated in motor recovery after experimental stroke (Jones and Schallert, 1992; Stroemer *et al.*, 1995; Nudo and Milliken, 1996; Li *et al.*, 1998; Carmichael *et al.*, 2001; Dijkhuizen *et al.*, 2001; Wei *et al.*, 2001; Zhang *et al.*, 2002). Our results suggest that reorganization of the human brain after stroke may also involve coupled structural and functional remodelling.

Among the ventral POG areas in which we observed co-localized structural and functional plasticity (ipsilesional putative areas 3b, 1 and 2; contralesional putative area 1), putative area 3b exhibited a significant linear correlation between cortical thickness and BOLD activation response in the patients. The BOLD activation response has been shown to scale roughly linearly with the extent of local neural processing (Logothetis *et al.*, 2001) and cerebral perfusion (Mandeville and Rosen, 2002). Therefore, the linear increase in the BOLD activation response observed in putative area 3b might have been due to an increase in stimulation-induced synaptic activity and capillary perfusion. That no other

ventral POG area or control cortical area exhibited a significant correlation between thickness and activation in the patients or controls suggests that these cortical parameters are not generally related. It is unclear why in the patients ventral POG areas other than putative area 3b did not exhibit a significant relationship between thickness and activation. One factor may relate to putative area 3b of the ventral POG being more closely linked to the hand region area 3b (primary somatosensory cortex) with neurovascular activity strongly connected to thalamic input, whereas the other ventral POG areas may be more closely associated with the higher-order somatosensory cortices with neurovascular activity reflecting a greater degree of cortico-cortical communication. An incremental change in the neural and non-neural elements associated with a cortical thickness increase in higher-order somatosensory cortices may relate poorly to their neurovascular response because of extensive cortico-cortical communication.

In conclusion, the findings of this study highlight the capacity of the adult human brain for structural and functional plasticity in association with motor recovery after stroke. These findings were made possible by the application of recently developed computational methods for high-resolution analysis of cortical activation patterns and cortical thickness from magnetic resonance images. Such findings expand our understanding of the spectrum of changes occurring in the brain after stroke in humans that may mediate restoration of function. It is hoped that an understanding of the full complement of restorative brain mechanisms will lead to the development of new therapeutic interventions that promote recovery after stroke in patients.

References

Anderson BJ, Eckburg PB, Relucio KI. Alterations in the thickness of motor cortical subregions after motor-skill learning and exercise. Learn Mem 2002; 9: 1–9.

Brodmann K. Localisation in the cerebral cortex. Garey LJ, translator. London: Smith-Gordon (original work published 1909); 1994.

Buonomano DV, Merzenich MM. Cortical plasticity: from synapses to maps. Annu Rev Neurosci 1998; 21: 149–86.

Burton H, MacLeod AM, Videen TO, Raichle ME. Multiple foci in parietal and frontal cortex activated by rubbing embossed grating patterns across fingerpads: a positron emission tomography study in humans. Cereb Cortex 1997; 7: 3–17.

Burton H, Abend NS, MacLeod AM, Sinclair RJ, Snyder AZ, Raichle ME. Tactile attention tasks enhance activation in somatosensory regions of

parietal cortex: a positron emission tomography study. Cereb Cortex 1999; 9: 662–74.

Calautti C, Leroy F, Guincestre JY, Baron JC. Displacement of primary sensorimotor cortex activation after subcortical stroke: a longitudinal PET study with clinical correlation. Neuroimage 2003; 19: 1650–4.

Carmichael ST, Wei L, Rovainen CM, Woolsey TA. New patterns of intracortical projections after focal cortical stroke. Neurobiol Dis 2001; 8: 910–22.

Carmichael ST, Archibeque I, Luke L, Nolan T, Momiy J, Li S. Growth-associated gene expression after stroke: evidence for a growth-promoting region in peri-infarct cortex. Exp Neurol 2005; 193: 291–311.

Cramer SC, Crafton KR. Somatotopy and movement representation sites following cortical stroke. Exp Brain Res 2006; 168: 25–32.

Cramer SC, Nelles G, Schaechter JD, Kaplan JD, Finklestein SP. Computerized measurement of motor performance after stroke. Stroke 1997a; 28: 2162–8.

Cramer SC, Nelles G, Benson RR, Kaplan JD, Parker RA, Kwong KK, et al. A functional MRI study of subjects recovered from hemiparetic stroke. Stroke 1997b; 28: 2518–27.

Cramer SC, Moore CI, Finklestein SP, Rosen BR. A pilot study of somatotopic mapping after cortical infarct. Stroke 2000; 31: 668–71.

Dale AM, Buckner RL. Selective averaging of rapidly presented individual trials using fMRI. Hum Brain Mapp 1999; 5: 329–40.

Dale AM, Fischl B, Sereno MI. Cortical surface-based analysis. I: Segmentation and surface reconstruction. Neuroimage 1999; 9: 179–94.

Diamond MC, Law F, Rhodes H, Lindner B, Rosenzweig MR, Krech D, et al. Increases in cortical depth and glia numbers in rats subjected to enriched environment. J Comp Neurol 1966; 128: 117–26.

Dijkhuizen RM, Ren J, Mandeville JB, Wu O, Ozdag FM, Moskowitz MA, et al. Functional magnetic resonance imaging of reorganization in rat brain after stroke. Proc Natl Acad Sci USA 2001; 98: 12766–71.

Elbert T, Rockstroh B. Reorganization of human cerebral cortex: the range of changes following use and injury. Neuroscientist 2004; 10: 129–41.

Fischl B, Dale AM. Measuring the thickness of the human cerebral cortex from magnetic resonance images. Proc Natl Acad Sci USA 2000; 97: 11050–5.

Fischl B, Sereno MI, Dale AM. Cortical surface-based analysis. II: Inflation, flattening, and a surface-based coordinate system. Neuroimage 1999a; 9: 196–207.

Fischl B, Sereno MI, Tootell RBH, Dale AM. High-resolution intersubject averaging and a coordinate system for the cortical surface. Hum Brain Mapp 1999b; 8: 272–84.

Fugl-Meyer AR, Jaasko L, Leyman I, Olsson S, Steglind S. The post-stroke hemiplegic patient: a method for the evaluation of physical performance. Scand J Rehabil Med 1975; 7: 13–31.

Gaser C, Schlaug G. Brain structures differ between musicians and non-musicians. J Neurosci 2003; 23: 9240–5.

Genovese CR, Lazar NA, Nichols T. Thresholding of statistical maps in functional neuroimaging using the false discovery rate. Neuroimage 2002; 15: 870–8.

Geyer S, Schleicher A, Zilles K. Areas 3a, 3b, and 1 of human primary somatosensory cortex. 1. Microstructural organization and interindividual variability. Neuroimage 1999; 10: 63–83.

Grefkes C, Geyer S, Schormann T, Roland P, Zilles K. Human somatosensory area 2: observer–independent cytoarchitectonic mapping, interindividual variability, and population map. Neuroimage 2001; 14: 617–31.

Han X, Jovicich J, Salat D, van der Kouwe A, Quinn B, Czanner S, et al. Reliability of MRI-derived measurements of human cerebral cortical thickness: the effects of field strength, scanner upgrade and manufacturer. Neuroimage, 2006; 32: 180–94.

Hickmott PW, Steen PA. Large-scale changes in dendritic structure during reorganization of adult somatosensory cortex. Nat Neurosci 2005; 8: 140–2.

Jang SH, Ahn SH, Yang DS, Lee DK, Kim DK, Son SM. Cortical reorganization of hand motor function to primary sensory cortex in hemiparetic patients with a primary motor cortex infarct. Arch Phys Med Rehabil 2005; 86: 1706–8.

Jones EG. Connectivity of the primate sensory-motor cortex. In: Peters A, Jones EG, editors. Cerebral cortex. New York: Plenum Press; 1986: p 113–84.

Jones TA, Schallert T. Overgrowth and pruning of dendrites in adult rats recovering from neocortical damage. Brain Res 1992; 581: 156–60.

Jones TA, Schallert T. Use-dependent growth of pyramidal neurons after neocortical damage. J Neurosci 1994; 14: 2140–52.

Kaas JH. What, if anything, is SI? Organization of first somatosensory area of cortex Physiol Rev 1983; 63: 206–31.

Killackey HP, Gould HJ 3rd, Cusick CG, Pons TP, Kaas JH. The relation of corpus callosum connections to architectonic fields and body surface maps in sensorimotor cortex of new and old world monkeys. J Comp Neurol 1983; 219: 384–419.

Kleim JA, Barbay S, Cooper NR, Hogg TM, Reidel CN, Remple MS, et al. Motor learning-dependent synaptogenesis is localized to functionally reorganized motor cortex. Neurobiol Learn Mem 2002; 77: 63–77.

Krubitzer L, Clarey JC, Tweedale R, Calford MB. Interhemispheric connections of somatosensory cortex in the flying fox. J Comp Neurol 1998; 402: 538–59.

Kuperberg GR, Broome MR, McGuire PK, David AS, Eddy M, Ozawa F, et al. Regionally localized thinning of the cerebral cortex in schizophrenia. Arch Gen Psychiatry 2003; 60: 878–88.

Li Y, Jiang N, Powers C, Chopp M. Neuronal damage and plasticity identified by microtubule-associated protein 2, growth-associated protein 43, and cyclin D1 immunoreactivity after focal cerebral ischemia in rats. Stroke 1998; 29: 1972–80.

Logothetis NK, Pauls J, Augath M, Trinath T, Oeltermann A. Neurophysiological investigation of the basis of the fMRI signal. Nature 2001; 412: 150–7.

Luft AR, Waller S, Forrester L, Smith GV, Whitall J, Macko RF, et al. Lesion location alters brain activation in chronically impaired stroke survivors. Neuroimage 2004; 21: 924–35.

Mandeville JB, Rosen BR. Functional MRI. In: Toga AW, Mazziotta JC, editors. Brain mapping: the methods. San Diego: Academic Press; 2002: p 315–49.

Medical Research Council (Great Britian). Aids to the examination of the peripheral nervous system. London: H M Stationery Office; 1976.

Meyer JR, Roychowdhury S, Russell EJ, Callahan C, Gitelman D, Mesulam MM. Location of the central sulcus via cortical thickness of the precentral and postcentral gyri on MR. AJNR Am J Neuroradiol 1996; 17: 1699–706.

Moore CI, Stern CE, Corkin S, Fischl B, Gray AC, Rosen BR, et al. Segregation of somatosensory activation in the human rolandic cortex using fMRI. J Neurophysiol 2000; 84: 558–69.

Nudo RJ, Milliken G. Reorganization of movement representations in primary motor cortex following focal ischemic infarcts in adult squirrel monkeys. J Neurophysiol 1996; 75: 2144–9.

Oldfield RC. The assessment and analysis of handedness: the Edinburgh Inventory. Neuropsychologia 1971; 9: 97–113.

Pineiro R, Pendlebury S, Johansen-Berg H, Matthews PM. Functional MRI detects posterior shifts in primary sensorimotor cortex activation after troke: evidence of local adaptive reorganization? Stroke 2001; 32: 1134–9.

Rademacher J, Burgel U, Geyer S, Schormann T, Schleicher A, Freund HJ, et al. Variability and asymmetry in the human precentral motor system. A cytoarchitectonic and myeloarchitectonic brain mapping study. Brain 2001; 124: 2232–58.

Rauch SL, Wright CI, Martis B, Busa E, McMullin KG, Shin LM, et al. A magnetic resonance imaging study of cortical thickness in animal phobia. Biol Psychiatry 2004; 55: 946–52.

Rosas HD, Liu AK, Hersch S, Glessner M, Ferrante RJ, Salat DH, et al. Regional and progressive thinning of the cortical ribbon in Huntington's disease. Neurology 2002; 58: 695–701.

Salat DH, Buckner RL, Snyder AZ, Greve DN, Desikan RS, Busa E, et al. Thinning of the cerebral cortex in aging. Cereb Cortex 2004; 14: 721–30.

Schaechter JD. Motor rehabilitation and brain plasticity after hemiparetic stroke. [Review]. Prog Neurobiol 2004; 73: 61–72.

Simpson W. The step method: a new adaptive psychophysical procedure. Percep Psychophys 1989; 45: 572–6.

Stern EB. Stability of the Jebson-Taylor Hand Function Test across three test sessions. Am J Occup Ther 1992; 46: 647–9.

Stroemer RP, Kent TA, Hulsebosch CE. Neocortical neural sprouting, synaptogenesis, and behavioral recovery after neocortical infarction in rats. Stroke 1995; 26: 2135–44.

Swain RA, Harris AB, Wiener EC, Dutka MV, Morris HD, Theien BE, et al. Prolonged exercise induces angiogenesis and increases cerebral blood volume in primary motor cortex of the rat. Neuroscience 2003; 117: 1037–46.

Thompson PM, Lee AD, Dutton RA, Geaga JA, Hayashi KM, Eckert MA, et al. Abnormal cortical complexity and thickness profiles mapped in Williams syndrome. J Neurosci 2005; 25: 4146–58.

Ward NS. Neural plasticity and recovery of function. Prog Brain Res 2005; 150: 527–35, [Review].

Wei L, Erinjeri JP, Rovainen CM, Woolsey TA. Collateral growth and angiogenesis around cortical stroke. Stroke 2001; 32: 2179–84.

Weiller C, Ramsay SC, Wise RJS, Friston KJ, Frackowiak RSJ. Individual patterns of functional reorganization in the human cerebral cortex after capsular infarction. Ann Neurol 1993; 33: 181–9.

Zemke AC, Heagerty PJ, Lee C, Cramer SC. Motor cortex organization after stroke is related to side of stroke and level of recovery. Stroke 2003; 34: e23–8.

Zhang ZG, Zhang L, Tsang W, Soltanian-Zadeh H, Morris D, Zhang R, et al. Correlation of VEGF and angiopoietin expression with disruption of blood–brain barrier and angiogenesis after focal cerebral ischemia. J Cereb Blood Flow Metab 2002; 22: 379–92.